Spin Blockade, Orbital Occupation, and Charge Ordering in $La_{1.5}Sr_{0.5}CoO_4$

C. F. Chang,[1] Z. Hu,[1] Hua Wu,[1] T. Burnus,[1] N. Hollmann,[1] M. Benomar,[1] T. Lorenz,[1] A. Tanaka,[2] H.-J. Lin,[3] H. H. Hsieh,[4] C. T. Chen,[3] and L. H. Tjeng[1]

[1]*II. Physikalisches Institut, Universität zu Köln, Zülpicher Strasse 77, 50937 Köln, Germany*
[2]*Department of Quantum Matter, ADSM, Hiroshima University, Higashi-Hiroshima 739-8530, Japan*
[3]*National Synchrotron Radiation Research Center, 101 Hsin-Ann Road, Hsinchu 30077, Taiwan*
[4]*Chung Cheng Institute of Technology, National Defense University, Taoyuan 335, Taiwan*

(Received 26 November 2008; published 16 March 2009)

Using Co-$L_{2,3}$ and O-K x-ray absorption spectroscopy, we reveal that the charge ordering in $La_{1.5}Sr_{0.5}CoO_4$ involves high spin ($S = 3/2$) Co^{2+} and low spin ($S = 0$) Co^{3+} ions. This provides evidence for the spin-blockade phenomenon as a source for the extremely insulating nature of the $La_{2-x}Sr_xCoO_4$ series. The associated e_g^2 and e_g^0 orbital occupation accounts for the large contrast in the Co-O bond lengths and, in turn, the high charge ordering temperature. Yet, the low magnetic ordering temperature is naturally explained by the presence of the nonmagnetic ($S = 0$) Co^{3+} ions. From the identification of the bands we infer that $La_{1.5}Sr_{0.5}CoO_4$ is a narrow band material.

DOI: 10.1103/PhysRevLett.102.116401 PACS numbers: 71.20.−b, 71.28.+d, 71.70.−d, 78.70.Dm

Considerable research effort has been spent on cobaltate materials during the last decade in search for new phenomena and extraordinary properties. A key aspect of cobaltates that distinguishes them from, e.g., the manganates and cuprates [1], is the spin state degree of freedom of the $Co^{3+/III}$ ions: it can be low spin (LS, $S = 0$), high spin (HS, $S = 2$), and even intermediate spin (IS, $S = 1$) [2,3]. This aspect comes on top of the orbital, spin (up or down) and charge degrees of freedom that already make the manganates and cuprates so exciting. Indeed, numerous cobaltate systems have been discovered with properties that include giant magnetoresistance [4,5], superconductivity [6] and ferro-ferri-antiferro-magnetic transitions with various forms of charge, orbital, and spin ordering [7–14]. A new and exciting aspect in here is the recognition that the so-called *spin-blockade* mechanism could be present and responsible for several of those unusual properties [15]. If true, this would open up new research opportunities since one could envision exploiting explicitly this mechanism in materials design.

Here we focus on the $La_{2-x}Sr_xCoO_4$ system, which shows quite peculiar transport and magnetic properties [16–25]. This material is extremely insulating for a very wide range of x values with anomalously high activation energies for conductivity, very much unlike the Mn, Ni, or Cu compounds [1,18,26]. The commensurate antiferromagnetic (AF) state remains stable up to a surprisingly high value of $x = 0.3$ [24,25]. Charge ordering (CO) and spin ordering (SO) at half doping involve quite different transition temperatures, namely $T_{CO} \sim 750$ K and $T_{SO} \leq 30$ K, respectively. This constitutes a ratio of 25, which is extraordinary since it is an order of magnitude larger than in the Mn and Ni materials [1,21,27].

It was reported that the SO in $La_{1.5}Sr_{0.5}CoO_4$ involves nonmagnetic (NM) Co^{3+} ions with the claim that these Co^{3+} ions are in the IS state and become NM due to strong planar anisotropy driven quenching of the spin angular momentum below the T_{SO} [21,22]. Here we go one step further. Using soft x-ray absorption spectroscopy (XAS) we are able to show unambiguously that the Co^{3+} ions are in the LS ($S = 0$) state, both below and above T_{SO}. Together with the verification that the Co^{2+} ions are HS ($S = 3/2$), we establish that the spin-blockade mechanism is active. The highly insulating character of the material over a wide range of temperatures is thus explained. Important is that the associated e_g^0 and e_g^2 orbital occupation ordering leads to a large difference in the Co-O bond lengths and the high T_{CO}. At the same time, the low T_{SO} follows naturally from the presence of the truly NM ($S = 0$) Co^{3+} ions.

Single crystals of $La_{1.5}Sr_{0.5}CoO_4$ have been grown by the travelling floating-zone method and characterized using magnetic and resistivity measurements [23]. The polarization-dependent XAS experiments were performed at the Dragon beam line of the National Synchrotron Radiation Research Center (NSRRC) in Taiwan. The Co-$L_{2,3}$ spectra were taken in the total electron yield (TEY) mode and the O-K also in the fluorescence yield (FY) mode with a photon energy resolution of 0.3 and 0.2 eV, respectively. The degree of linear polarization of the incident light was 99%. The crystals were mounted with the **c** axis perpendicular to the Poynting vector of the light. By rotating the sample around this Poynting vector, the polarization of the electric field can be varied continuously from $\mathbf{E} \parallel \mathbf{c}$ to $\mathbf{E} \perp \mathbf{c}$. The crystals were cleaved parallel to the **c** axis in a vacuum of 10^{-10} mbar.

Figure 1 depicts the room temperature isotropic Co-$L_{2,3}$ XAS spectrum of $La_{1.5}Sr_{0.5}CoO_4$ together with those of Sr_2CoO_3Cl, $EuCoO_3$, and CoO serving as the HS-Co^{3+}, the LS-Co^{3+}, and the HS-Co^{2+} references, respectively [28]. The spectra are dominated by the Co $2p$ core-hole spin-orbit coupling which splits the spectrum roughly in

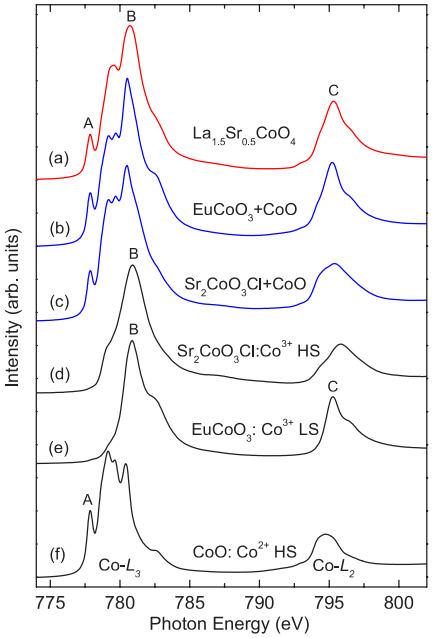

FIG. 1 (color online). Isotropic Co-$L_{2,3}$ XAS spectra of (a) $La_{1.5}Sr_{0.5}CoO_4$, (b) the HS-CoO plus LS-$EuCoO_3$ scenario, (c) the HS-CoO plus HS-Sr_2CoO_3Cl scenario, (d) Sr_2CoO_3Cl, (e) $EuCoO_3$, and (f) CoO, all taken at 300 K.

two parts, namely, the L_3 ($h\nu \approx 776$–784 eV) and L_2 ($h\nu \approx 793$–797 eV) white lines regions. The line shape strongly depends on the multiplet structure given by the Co $3d$-$3d$ and $2p$-$3d$ Coulomb and exchange interactions, as well as by the local crystal fields and the hybridization with the O $2p$ ligands. Unique to soft XAS is that the dipole selection rules are very sensitive in determining which of the $2p^5 3d^{n+1}$ final states can be reached and with what intensity, starting from a particular $2p^6 3d^n$ initial state ($n = 6$ for Co^{3+} and $n = 7$ for Co^{2+}) [29,30]. This makes the technique extremely sensitive to the symmetry of the initial state, i.e., the spin, orbital and valence states of the ions [28,31–35].

The spectra of the reference samples show quite different multiplet structures. In particular, the lowest energy peak (A) of the CoO at 777.8 eV is characteristic for an octahedral Co^{2+} since it has an energy well below that of any Co^{3+} or Co^{4+} (not shown here) features. Also very characteristic is the dominant peak (B) at 781 eV of a Co^{3+} ion. Compared to the HS Sr_2CoO_3Cl, the LS $EuCoO_3$ has a higher intensity at the L_2 edge with a rather sharp peak (C) at 795 eV. Focussing now on the $La_{1.5}Sr_{0.5}CoO_4$ spectrum, one can clearly observe, among others, the low energy peak (A), the dominant peak (B), and the spectral feature (C). This strongly hints towards the presence of not only Co^{2+} and Co^{3+} ions in this material, but especially that the Co^{3+} is LS. To verify this, we have carried out a simple simulation by making a superposition of the as-measured CoO and $EuCoO_3$ spectra and compare the result with the spectrum of $La_{1.5}Sr_{0.5}CoO_4$. We see from Fig. 1 that the simulation is almost perfect. As a counter check, we also made a superposition of the CoO and Sr_2CoO_3Cl spectra, and find it to be different from the spectrum of $La_{1.5}Sr_{0.5}CoO_4$, especially in the L_2 edge region.

In order to further confirm that the Co^{3+} ions are in the LS state, we have measured the polarization dependence of the Co-$L_{2,3}$ XAS of $La_{1.5}Sr_{0.5}CoO_4$ and have simulated the spectra using the successful configuration interaction cluster model that includes the full atomic multiplet theory and the hybridization with the O $2p$ ligands [29,30]. For this we use parameter values typical for Co^{2+} and Co^{3+} systems [28,32,33,36]. The Co $3d$ to O $2p$ transfer integrals were adapted for the various Co-O bond lengths [37] according to Harrison's prescription [38]. The crystal field parameters were determined from constrained density-functional calculations using the linearized augmented plane wave plus local orbital method [39] and the electron-correlation corrected local-density-approximation (LDA + U with $U = 5$ eV) [40]. The cluster model calculations were done using XTLS 8.3 [30].

The top panel of Fig. 2(a) shows the experimental Co-$L_{2,3}$ XAS of $La_{1.5}Sr_{0.5}CoO_4$ taken with $\mathbf{E} \parallel \mathbf{c}$ (red) and $\mathbf{E} \perp \mathbf{c}$ (black). The experimental linear dichroic (LD) signal, defined as the difference between two polarizations, is displayed in the middle panel (magenta), to-

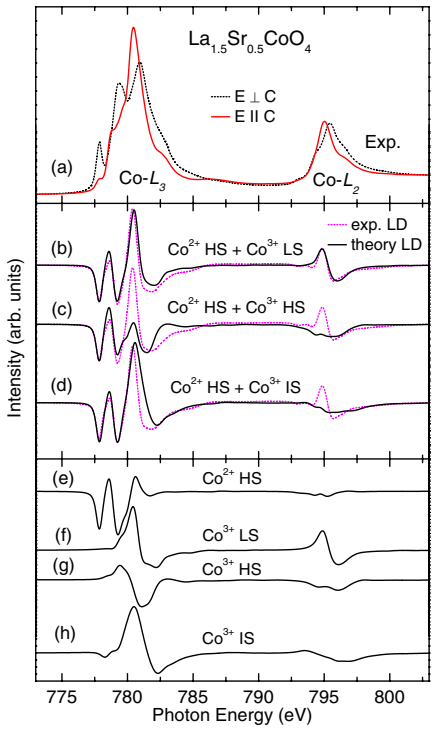

FIG. 2 (color online). (a) Experimental polarization-dependent Co-$L_{2,3}$ XAS of $La_{1.5}Sr_{0.5}CoO_4$ for $\mathbf{E} \parallel \mathbf{c}$ (red line) and $\mathbf{E} \perp \mathbf{c}$ (black dotted line); (b), (c), and (d) the experimental linear dichroism (magenta dotted lines) together with the theoretical one (black lines) calculated for scenarios with HS-Co^{2+} and LS-, HS-, or IS-Co^{3+}, respectively. The calculated linear dichroism for the HS-Co^{2+}, LS-, HS-, and IS-Co^{3+} is also shown individually in (e), (f), (g), and (h).

gether with the simulated LD spectra (black) for the Co^{3+} ion in the (b) LS, (c) HS, and (d) IS state, respectively, while the Co^{2+} ion is kept in the HS. One can observe from the middle panel that the LS-Co^{3+} scenario nicely reproduces all features of the experimental LD spectrum. In contrast, the HS-Co^{3+} assumption would lead to significant discrepancies, not only at the L_3 but also at the L_2 edge. Also the IS-Co^{3+} scenario gives less satisfactory fit to the experimental spectrum: the L_2 edge structure cannot be reproduced at all. More insight can be gained from the lower panel of Fig. 2 in which the calculated LD spectra are individually depicted. The Co^{2+} LD spectrum (e) shows only a modest modulation at the L_2 edge, and so does the HS-Co^{3+} (g) and the IS-Co^{3+} (h) as well. Only the LS-Co^{3+} (f) displays the strong LD modulation as experimentally observed for the L_2 region.

So far the Co^{3+} spin state in $La_{2-x}Sr_xCoO_4$ has been studied using magnetic susceptibility [16–18,23] or NMR measurements [20], with conflicting results: all three possible scenarios (HS, IS, LS) have been proposed. Interestingly, neutron scattering experiments have revealed the presence of NM Co^{3+} in the SO state of $La_{1.5}Sr_{0.5}CoO_4$ [21]. Yet it was claimed that these Co^{3+} ions are in the IS state and that they become NM as a result of the quenching of the spin angular momentum due to the strong planar anisotropy in the SO state [21,22].

Our XAS data yield new and crucial information. The Co^{3+} ions are indeed NM, but because of a completely different reason: they are in the LS ($S = 0$) state. The XAS data were taken at room temperature, i.e., above T_{SO}. We expect that this LS ($S = 0$) state is also stable below T_{SO}. We have verified this using yet another spectroscopic method, namely, the O-K XAS. The top panel of Fig. 3(a) displays the isotropic spectra of $La_{1.5}Sr_{0.5}CoO_4$ taken at 300 K and 18 K. These spectra were taken in the FY method to avoid charging problems which otherwise could occur at low sample temperatures when using the TEY. One can clearly see that the line shape of the 529.5 eV pre-edge feature at both temperatures is very similar to that of $EuCoO_3$, a reliable LS-Co^{3+} reference [28]. The temperature dependence, if any, is only a slight broadening, and certainly not the massive change of the spectral line shape (over a range of ≈ 1 eV) as reported for $LaCoO_3$ in going from the low-temperature NM to the high-temperature paramagnetic state [31].

The presence of LS-Co^{3+} ions provides a natural explanation for the rapid lowering of the T_{SO} when doping La_2CoO_4 with Sr. The number of paths with strong superexchange interactions between the HS-Co^{2+} ions is simply reduced when NM Co^{3+} ions are introduced. It should therefore be of no surprise that the T_{SO} drops from 275 K for La_2CoO_4 to only 30 K for $La_{1.5}Sr_{0.5}CoO_4$ in which the Co^{2+}/Co^{3+} ions are checkerboard ordered.

The presence of LS-Co^{3+} ions in between HS-Co^{2+} is also exciting since it gives a beautiful explanation for the highly insulating behavior in $La_{2-x}Sr_xCoO_4$ despite the heavy doping. If one considers a pair of neighboring

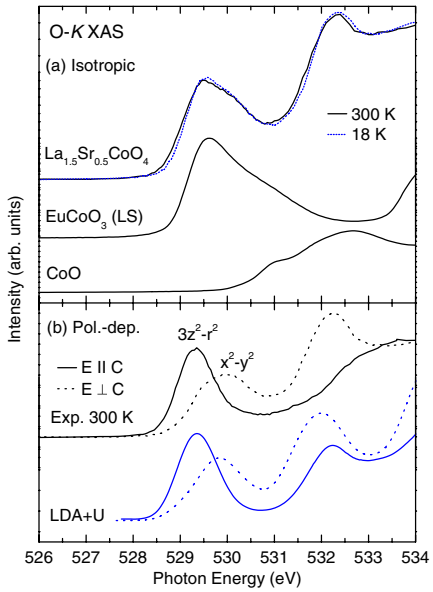

FIG. 3 (color online). (a) Isotropic O-K XAS of $La_{1.5}Sr_{0.5}CoO_4$ taken at 18 K (blue dotted line) and 300 K (black solid line), together with those of $EuCoO_3$ (LS) and CoO. (b) Polarization-dependent O-K XAS, taken with $\mathbf{E} \parallel \mathbf{c}$ (solid line) and $\mathbf{E} \perp \mathbf{c}$ (dotted line), together with the LDA + U unoccupied O $2p$ density of states (blue curves).

HS-Co^{2+} ($S = 3/2$) and LS-Co^{3+} ($S = 0$) ions, one can directly see that the hopping of a charge carrier will not result in an identical pair with just the charges interchanged. Instead, the pair created will have a completely different spin state configuration: the hopping of a spin $1/2$ particle will produce an IS-Co^{3+} ($S = 1$) and LS-Co^{2+} ($S = 1/2$) final state. Although such a hopping does not involve the Coulomb energy U, it does cost a significant amount of energy since the energy difference between a HS- and LS-Co^{2+} as well as between a LS- and IS-Co^{3+} could amount to several tenths of an eV [2]. The hopping of charge carriers between these two types of Co ions is thus severely suppressed. This type of suppression of the conductivity, known as spin-blockade, has been proposed to explain the thermoelectric power of $HoBaCo_2O_{5.5}$ [15]. We note that the spin-blockade mechanism is effective in $La_{1.5}Sr_{0.5}CoO_4$ both below and above the T_{SO} since the LS state of the Co^{3+} is independent of the SO. This explains why the activation energies for the conductivity remain high even at elevated temperatures.

The spin state contrast, which goes along with the Co^{2+}/Co^{3+} charge state, has also consequences for the stability of the CO. The orbital occupation of the HS-Co^{2+} is predominantly $t_{2g}^5 e_g^2$ while that of the LS-Co^{3+} is mainly $t_{2g}^6 e_g^0$, as we have verified from our cluster calculations. There is thus also an extremely strong e_g orbital occupation contrast, even when taking into account that the LS-Co^{3+} is more covalent than the HS-Co^{2+} [41]. With the e_g orbitals pointing towards the oxygens and the t_{2g} in between, this leads to significant differences in the local

Co-O distances for the two different ions, as indeed revealed by diffraction experiments [21,24,25]. This in turn causes strong localization and stabilization of the charge contrast, thereby explaining the very high $T_{CO} \sim 750$ K in $La_{1.5}Sr_{0.5}CoO_4$.

There is yet another aspect which makes this system to be highly insulating. For this we look in more detail at the energetics of the unoccupied states of the Co^{3+}. The bottom panel of Fig. 3(b) shows the polarization dependence of the O-K XAS. Here we are mainly interested in the lowest lying states, i.e., the unoccupied states of the Co^{3+} which can be reached when an electron is transferred from a neighboring Co^{2+}. These states are located in the so-called pre-edge region between 528–531 eV [31]. Using $\mathbf{E} \parallel \mathbf{c}$ light (solid line) we can reach the unoccupied O-$2p_z$ − Co-$3d_{3z^2-r^2}$ hybridized band, and found it to be peaked at 529.3 eV. With $\mathbf{E} \perp \mathbf{c}$ light (dotted line), we see that the peak of the mixed O-$2p_{x,y}$ − Co-$3d_{x^2-y^2}$ band lies 0.7 eV higher, at 530.0 eV. The lowest energy states at 528.5 eV are of almost pure $3z^2 - r^2$ nature. These assignments are very well supported by the LDA + U calculations: not only the higher intensity of the $3z^2 - r^2$ (solid line) in comparison to that of the $x^2 - y^2$ state (dotted line) is reproduced but also the relative energy positions.

This is an important finding since it establishes that the conduction-band bottom is of $3z^2 - r^2$ origin. This is very different from the cuprate, nickelate, and manganate systems, where the relevant band is formed out of the $x^2 - y^2$ orbital. The consequences are obvious: with the $3z^2 - r^2$ orbital having much smaller overlap with the in-plane O-$2p_{x,y}$ ligands than the $x^2 - y^2$, the conduction band gets much narrower, with the result that the spin-blockade effect together with the strong coupling of the Co-O distances with the charge or spin state of the Co ions become the dominant interactions to make $La_{2-x}Sr_xCoO_4$ highly insulating over a wide range of x.

We note that the observed and calculated 0.7 eV energy shift between the $3z^2 - r^2$ and the $x^2 - y^2$ states in Fig. 3(b) reflects the large tetragonal distortion of about 10% [37]. This large e_g crystal field splitting is in fact the cause for the strong modulation in the LD spectrum at the L_2 edge for the LS-Co^{3+} ion as depicted in the bottom panel of Fig. 2, curve (f); without such an energy splitting which is felt by the electron promoted from the Co $2p$ core, one would not observe any dichroism in the otherwise highly symmetric, closed-shell t_{2g}^6 ground state.

To summarize, we find using the Co-$L_{2,3}$ and O-K XAS that the charge ordering in $La_{1.5}Sr_{0.5}CoO_4$ involves high spin ($S = 3/2$) Co^{2+} and low spin ($S = 0$) Co^{3+} ions. We infer that the spin-blockade mechanism is active here and that there is a strong coupling between the local Co-O distances and the charge/spin state of the ions. The crystal field scheme for the Co^{3+} ion caused by the tetragonal distortion makes the conduction band extremely narrow. All these factors provide an explanation for the highly insulating properties as well as for the very low T_{SO} and the exceptionally high T_{CO}.

We thank Lucie Hamdan and Matthias Cwik for their skillful technical assistance. This work is supported by the Deutsche Forschungsgemeinschaft through SFB 608.

[1] M. Imada *et al.*, Rev. Mod. Phys. **70**, 1039 (1998).
[2] S. Sugano *et al.*, *Multiplets of Transition-Metal Ions in Crystals* (Academic, New York, 1970).
[3] J. B. Goodenough, in *Progress in Solid State Chemistry*, edited by H. Reiss (Pergamon, Oxford, 1971), Vol. 5.
[4] G. Briceño *et al.*, Science **270**, 273 (1995).
[5] C. Martin *et al.*, Appl. Phys. Lett. **71**, 1421 (1997).
[6] K. Takada *et al.*, Nature (London) **422**, 53 (2003).
[7] H. Fjellvåg *et al.*, J. Solid State Chem. **124**, 190 (1996).
[8] T. Vogt *et al.*, Phys. Rev. Lett. **84**, 2969 (2000).
[9] S. Loureiro *et al.*, Chem. Mater. **12**, 3181 (2000).
[10] S. Niitaka *et al.*, Phys. Rev. Lett. **87**, 177202 (2001).
[11] J. C. Burley *et al.*, J. Solid State Chem. **170**, 339 (2003).
[12] A. A. Taskin *et al.*, Phys. Rev. Lett. **90**, 227201 (2003).
[13] Y. B. Kudasov, Phys. Rev. Lett. **96**, 027212 (2006).
[14] H. Luetkens *et al.*, Phys. Rev. Lett. **101**, 017601 (2008).
[15] A. Maignan *et al.*, Phys. Rev. Lett. **93**, 026401 (2004).
[16] K. G. Srivastava, Phys. Lett. **4**, 55 (1963).
[17] T. Matsuura *et al.*, J. Phys. Chem. Solids **49**, 1403 (1988); **49**, 1409 (1988).
[18] Y. Moritomo *et al.*, Phys. Rev. B **55**, R14 725 (1997).
[19] E. Iguchi *et al.*, J. Solid State Chem. **139**, 176 (1998).
[20] M. Itoh *et al.*, Physica (Amsterdam) **259–261B**, 997 (1999).
[21] I. A. Zaliznyak *et al.*, Phys. Rev. Lett. **85**, 4353 (2000).
[22] I. A. Zaliznyak *et al.*, Phys. Rev. B **64**, 195117 (2001).
[23] N. Hollmann *et al.*, New J. Phys. **10**, 023018 (2008).
[24] M. Cwik *et al.*, Phys. Rev. Lett. **102**, 057201 (2009).
[25] N. Sakiyama *et al.*, Phys. Rev. B **78**, 180406(R) (2008).
[26] C. N. Munnings *et al.*, Solid State Ionics **177**, 1849 (2006).
[27] R. Kajimoto *et al.*, Phys. Rev. B **67**, 014511 (2003).
[28] Z. Hu *et al.*, Phys. Rev. Lett. **92**, 207402 (2004).
[29] F. M. F. de Groot, J. Electron Spectrosc. Relat. Phenom. **67**, 529 (1994).
[30] A. Tanaka and T. Jo, J. Phys. Soc. Jpn. **63**, 2788 (1994).
[31] M. Abbate *et al.*, Phys. Rev. B **47**, 16 124 (1993).
[32] M. W. Haverkort *et al.*, Phys. Rev. Lett. **97**, 176405 (2006).
[33] T. Burnus *et al.*, Phys. Rev. B **74**, 245111 (2006).
[34] S. I. Csiszar *et al.*, Phys. Rev. Lett. **95**, 187205 (2005).
[35] C. Mitra *et al.*, Phys. Rev. B **67**, 092404 (2003).
[36] Co^{2+} parameters [eV]: $U_{dd} = 6.5$, $U_{cd} = 8.2$, $\Delta = 6.5$, $10Dq = 0.525$, $\Delta_{e_g} = 0.18$, $\Delta_{t_{2g}} = 0.03$, $pd\sigma_{x,y} = -1.43$, $pd\sigma_z = -0.96$; Co^{3+}: $U_{dd} = 5.5$, $U_{cd} = 7.0$, $\Delta = 3.5$, $10Dq = 0.785$, $\Delta_{e_g} = 0.24$, $\Delta_{t_{2g}} = 0.07$, $pd\sigma_{x,y} = -1.61$, $pd\sigma_z = -1.16$.
[37] M. Cwik, Ph.D. thesis, Universität zu Köln, 2007.
[38] W. A. Harrison, *Electronic Structure and the Properties of Solids* (Dover, New York, 1989).
[39] P. Blaha *et al.*, WIEN2K package, http://www.wien2k.at.
[40] V. I. Anisimov *et al.*, Phys. Rev. B **48**, 16 929 (1993).
[41] T. Saitoh *et al.*, Phys. Rev. B **55**, 4257 (1997).